Two-Stage Reduction of H_2–Air Kinetics for CFD: Sensitivity Pruning and Multi-Objective Rate Optimisation

G. Cinieri*, N. Yalynskaya*,M. B. Chandio*, Z. A. Shah*, G. Mehdi, O. Kaario**, M.G. De Giorgi***
mariagrazia.degiorgi@unisalento.it
*University of Salento, Lecce, IT
**University of Aalto, Espoo, FI

Abstract
A reduced kinetic modelling framework for H2–air combustion is developed in view of computationally heavy applications, as CFD studies. Four detailed H_2 oxidation mechanisms are systematically validated against laminar burning velocity (S_L) and ignition delay time (IDT) targets, and the Li (2007) mechanism is retained as the reduction baseline for its best agreement with elevated-pressure IDT data and a small number of reactions. Mechanism validation covers $\Phi \in [0.3–3.0]$ at 1 atm, 298 K for S_L and stoichiometric H_2/air at 10–70 bar for IDT, while optimization is performed on $\Phi \in [0.5–1.5]$ at 1 bar and $T \in [1000, 1500]$ K. A two-stage workflow is then applied: an IDT-based sensitivity pruning yields a 10-reaction skeletal mechanism, after which NSGA-III multi-objective optimisation in pyMechOpt calibrates the rate coefficients within ±10% to recover flame-speed accuracy, reducing the S_L MAPE. Among the four optimised candidates, Opt Model 3 offers the best IDT–SL compromise across the investigated range for equivalence ratios close to stoichiometric.

1. Introduction

H_2 combustion is a key pathway for low-carbon propulsion and energy-conversion systems, but its predictive modelling remains challenging because H_2 flames are highly sensitive to kinetic, transport, and thermodynamic properties. Including detailed plasma-combustion chemistry in multidimensional CFD is computationally expensive because of complicated plasma chemistry and timescale separation stiffness. At the same time, overly reduced mechanisms may lose accuracy in key combustion observables such as S_L, IDT, and radical formation. This work develops a new CFD-oriented reduced kinetic framework for H_2 combustion.

2. Methodology

Four detailed H2 oxidation mechanisms were considered: Li et al. (2007) [1], Li et al. (2015) [2], the San Diego mechanism (2016) [3], and Konnov et al. (2019) [4]. Each mechanism was assessed against S_L (Alekseev et al. [5], p = 1 atm, T = 298 K, diluted $H_2/N_2–O_2$/He mixture; composition in Figure 1 caption) and IDT (Das et al. [6], stoichiometric H_2/air at 10, 30, 70 bar). IDT was computed in Cantera with a 0D adiabatic constant-volume reactor, defined as the time to maximum d[OH]/dt. Predictive accuracy is quantified by the MAPE (eq. 1):

$$MAPE = \left(\frac{100}{N}\right) * \Sigma_{i=1}^{N} \left| \frac{\left(y_i^{model} - y_i^{exp}\right)}{y_i^{exp}} \right| \quad (1)$$

As depicted in Figure 1, Li et al. (2007) was selected as the reduction baseline because, within the considered mechanisms, it best matched the selected elevated-pressure IDT data while remaining relatively compact. For S_L, the lowest error is achieved by Li et al. (2015), with a MAPE of approximately 9%, whereas the highest error is observed for Li et al. (2007), with

a MAPE of approximately 21%.

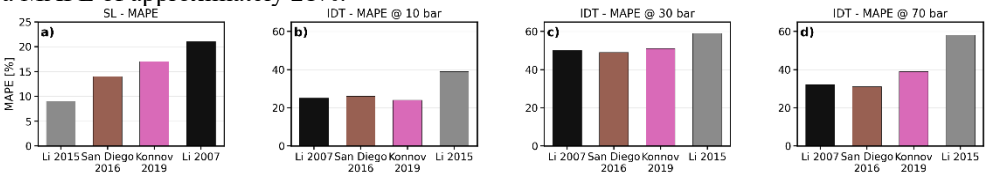

Figure 1. S_L at p=1 atm, T=298 K 25:75 (H_2 + N_2) fuel composition with 12.5:87.5 (O_2 + He) oxidizer composition. Experimental data by Alekseev et al. *[5]* , IDT vs Das et al. *[6]* experimental data at stoichiometric mixture for different initial pressure: b) 10 bar; c) 30 bar; d) 70 bar.

Since Li2007 shows the best IDT performance and the worst on SL, a two-stage reduction workflow — sensitivity-based pruning followed by evolutionary rate optimization — was adopted to obtain a CFD-suitable mechanism preserving IDT and SL over the target domain. Stage 1. IDT-based reaction pruning. A greedy backward-elimination procedure was performed in Cantera (0D adiabatic constant-volume reactor) over T={1400,1500,…,2200} K, P={1,2,10} bar, Φ={0.8,1.0,1.2}. Reactions were ranked by IDT sensitivity to their rate coefficients and removed iteratively; each removal was accepted only if IDT errors remained below 10% max and 5% mean, with at least 60% valid ignition cases. This yielded a 10-reaction skeletal mechanism.

Table 1. Ten-reaction skeletal H_2 oxidation mechanism retained from the Li(2007)-based mechanism.

No.	Conserved reaction from Li-based 10-reaction model	Reaction type
1	$H + O_2 \rightleftharpoons O + OH$	Elementary
2	$H_2 + O \rightleftharpoons H + OH$	Elementary
3	$H_2 + OH \rightleftharpoons H + H_2O$	Elementary
4	$H + OH + M \rightleftharpoons H_2O + M$	Three-body
5	$H + O_2 (+M) \rightleftharpoons HO_2 (+M)$	Falloff
7	$H + HO_2 \rightleftharpoons 2\ OH$	Elementary
8	$2\ HO_2 \rightleftharpoons H_2O_2 + O_2$	Elementary
9	$H_2O_2 (+M) \rightleftharpoons 2\ OH (+M)$	Falloff
10	$H + H_2O_2 \rightleftharpoons H_2 + HO_2$	Elementary

Stage 2. Multi-objective evolutionary optimization. The skeletal mechanism in Table 1 was calibrated with pyMechOpt [7]. Training was performed at 1 bar for six conditions: two temperatures (1000 K,1500 K) and three equivalence ratios (0.5, 1.0, 1.5). The algorithm was run with $pop_{size} = 25$ and $max_{gen} = 50$. The objective combined integral constraints on major species (H2, O2, H2O) with peak-behavior constraints on radicals (OH, HO2), enforcing both global conversion and chain-branching/low-temperature pathways.

3. Results

The optimization was driven primarily by the S_L error, since IDT accuracy is already preserved by the Stage 1 skeletal reduction. The four generated mechanisms therefore share the same 10 reactions; their rate coefficients are reported in Figure 2 as percentage variations relative to the baseline mechanism.

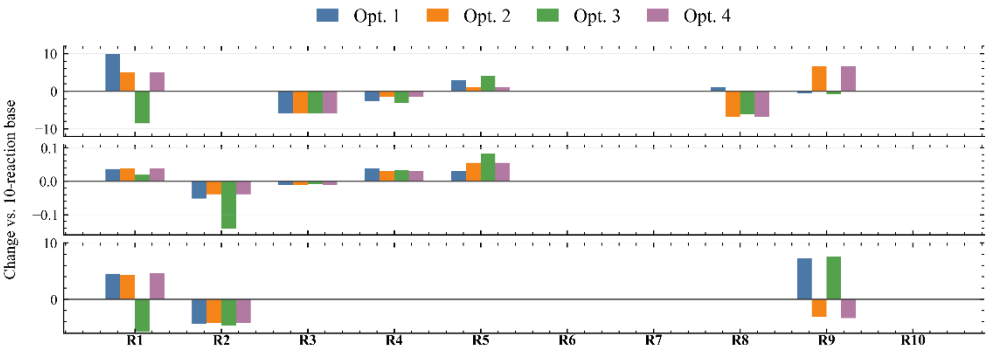

Figure 2. Percentage change of the Arrhenius coefficients of the 10 reactions in Table1 relative to the original Li (2007) mechanism a) A, b) b, c) E_a.

All optimized candidates (Opt Models1-4) exhibit a substantial improvement relative to the 10-reaction baseline, reducing the mean absolute percentage. The predictive capability of the reduced and optimized mechanisms was further assessed through the mean absolute percentage error (MAPE) with respect to the available experimental data in Figure 3. For ignition delay times, the comparison was performed against the measurements of Das et al. [6] over the available pressure range, while for laminar flame speed the comparison was performed against the data of Alekseev et al. [5]. The optimized mechanisms introduce a moderate increase in IDT error, which reflects the trade-off associated with improving the laminar flame speed response while retaining a compact kinetic structure. For laminar flame speed, the MAPE was evaluated as a function of equivalence ratio. In this case, the optimized mechanisms significantly reduce the error compared with the 10-reaction model over most of the investigated range, especially near stoichiometric and moderately rich conditions. Overall, the two error surfaces highlight the compromise between ignition-delay preservation and flame-speed correction, with the optimized mechanisms providing improved flame propagation accuracy at the cost of a limited degradation in IDT prediction. As summarized in Table 2, the 10-reaction baseline shows a mean SL MAPE of 61.9%, which the optimized variants reduce to 32.8–39.6%, while the IDT mean MAPE only moderately increases from 35.3% to 37.6–39.8%.

Table 2. Mean and best-case MAPE for IDT (against Das et al. [6] at ϕ=1, p=10, 30, 70 bar) and S_L (against Alekseev et al. [5] as a function of ϕ at 1 bar) for the investigated mechanisms.

Mechanism	*IDT mean MAPE (%)*	*Best IDT case*	*Best IDT MAPE (%)*	*SL mean MAPE (%)*	*Best SL case*	*Best SL MAPE (%)*
Li detailed	*35.2*	*10 bar*	*26.9*	*21.0*	*ϕ = 1.30*	*8.3*
10-reaction model	*35.3*	*10 bar*	*24.4*	*61.9*	*ϕ = 1.19*	*36.3*
Opt. Model 1	*38.9*	*10 bar*	*26.8*	*37.0*	*ϕ = 1.10*	*19.9*
Opt. Model 2	*39.8*	*10 bar*	*24.4*	*33.4*	*ϕ = 1.10*	*19.6*
Opt. Model 3	*37.6*	*10 bar*	*30.9*	*39.6*	*ϕ = 0.80*	*14.0*
Opt. Model 4	*39.5*	*10 bar*	*23.9*	*32.8*	*ϕ = 1.10*	*18.9*

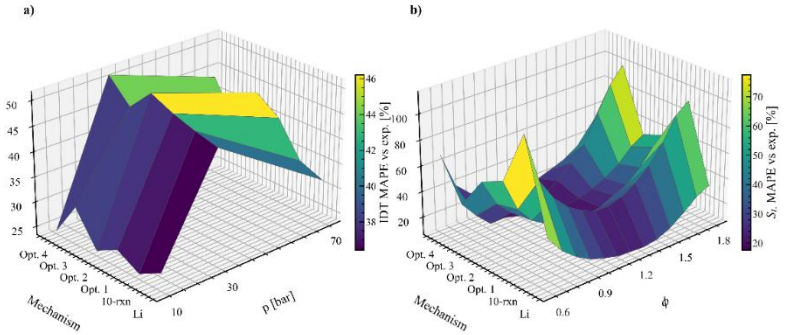

Figure 3. Mean absolute percentage error (MAPE) of the investigated mechanisms with respect to experimental data: a) IDT MAPE against Das et al. [6] at ϕ=1 for p=10, 30, 70 bar; b) S_L MAPE against Alekseev et al. [5] as a function of ϕ at 1 bar.

4. Conclusions

A two-stage reduction workflow — IDT-based sensitivity pruning of the Li (2007) mechanism followed by NSGA-III rate calibration within ±10% — yields a 10-reaction skeletal model for CFD-oriented H_2–air combustion. Opt Model 3 provides the best IDT–SL compromise, reducing the mean SL MAPE from 61.9% (10-reaction baseline) to 39.6% — especially near stoichiometric and moderately rich conditions — at the cost of a limited degradation in IDT accuracy (37.6% vs. 35.3%). Opt Model 4 attains the lowest mean S_L MAPE overall (32.8%).

Acknowledgements

Funded by the European Union

This work was provided within the framework of the FFLECS Project funded by the European Union's Horizon Europe research and Innovation programme under Grant Agreement No 101096436 (CUP F83C23003480006).

The authors also acknowledge financial support under ICHAruS, funded by the European Union under the Horizon Europe — HORIZON-MSCA-2022-DN-01 (Marie Skłodowska-Curie Doctoral Networks) programme, Grant Agreement No. 101120321. Funded by the European Union. For both projects, views and opinions expressed are, however, those of the author(s) only and do not necessarily reflect those of the European Union or the granting authority. Neither the European Union nor the granting authority can be held responsible for them.

References

[1] 'A comprehensive kinetic mechanism for CO, CH2O, and CH3OH combustion - Li - 2007 - International Journal of Chemical Kinetics - Wiley Online Library'. Accessed: Jan. 09, 2026. [Online]. Available: https://onlinelibrary.wiley.com/doi/10.1002/kin.20218

[2] X. Li, X. You, F. Wu, and C. K. Law, 'Uncertainty analysis of the kinetic model prediction for high-pressure H2/CO combustion', *Proceedings of the Combustion Institute*, vol. 35, no. 1, pp. 617–624, Jan. 2015, doi: 10.1016/j.proci.2014.07.047.

[3] 'Chemical Mechanism: Combustion Research Group at UC San Diego'. Accessed: Oct. 28, 2023. [Online]. Available: https://web.eng.ucsd.edu/mae/groups/combustion/mechanism.html

[4] A. A. Konnov, 'Yet another kinetic mechanism for hydrogen combustion', *Combustion and Flame*, vol. 203, pp. 14–22, May 2019, doi: 10.1016/j.combustflame.2019.01.032.

[5] V. A. Alekseev, M. Christensen, and A. A. Konnov, 'The effect of temperature on the adiabatic burning velocities of diluted hydrogen flames: A kinetic study using an updated mechanism', *Combustion and Flame*, vol. 162, no. 5, pp. 1884–1898, May 2015, doi: 10.1016/j.combustflame.2014.12.009.

[6] A. K. Das, C.-J. Sung, Y. Zhang, and G. Mittal, 'Ignition delay study of moist hydrogen/oxidizer mixtures using a rapid compression machine', *International Journal of Hydrogen Energy*, vol. 37, no. 8, pp. 6901–6911, Apr. 2012, doi: 10.1016/j.ijhydene.2012.01.111.

[7] S. Di, N. Yu, S. Han, and H. He, 'pyMechOpt: A Python toolbox for optimizing of reaction mechanisms', *SoftwareX*, vol. 29, p. 102001, Feb. 2025, doi: 10.1016/j.softx.2024.102001.